J. Fluid Mech. (2009), *vol.* 638, *pp.* 73–93.
doi:10.1017/S002211200999084X

On the logarithmic mean profile

J. KLEWICKI[1]†, P. FIFE[2] AND T. WEI[3]

[1]Department of Mechanical Engineering, University of New Hampshire, Durham, NH 03824, USA

[2]Department of Mathematics, University of Utah, Salt Lake City, UT 84112, USA

[3]Department of Mechanical Engineering, Pennsylvania State University, University Park, PA 16802, USA

(Received 15 January 2009; revised 16 June 2009; accepted 16 June 2009; first published online 23 September 2009)

Elements of the first-principles-based theory of Wei *et al.* (*J. Fluid Mech.*, vol. 522, 2005, p. 303), Fife *et al.* (*Multiscale Model. Simul.*, vol. 4, 2005*a*, p. 936; *J. Fluid Mech.*, vol. 532, 2005*b*, p. 165) and Fife, Klewicki & Wei (*J. Discrete Continuous Dyn. Syst.*, vol. 24, 2009, p. 781) are clarified and their veracity tested relative to the properties of the logarithmic mean velocity profile. While the approach employed broadly reveals the mathematical structure admitted by the time averaged Navier–Stokes equations, results are primarily provided for fully developed pressure driven flow in a two-dimensional channel. The theory demonstrates that the appropriately simplified mean differential statement of Newton's second law formally admits a hierarchy of scaling layers, each having a distinct characteristic length. The theory also specifies that these characteristic lengths asymptotically scale with distance from the wall over a well-defined range of wall-normal positions, y. Numerical simulation data are shown to support these analytical findings in every measure explored. The mean velocity profile is shown to exhibit logarithmic dependence (exact or approximate) when the solution to the mean equation of motion exhibits (exact or approximate) self-similarity from layer to layer within the hierarchy. The condition of pure self-similarity corresponds to a constant leading coefficient in the logarithmic mean velocity equation. The theory predicts and clarifies why logarithmic behaviour is better approximated as the Reynolds number gets large. An exact equation for the leading coefficient (von Kármán coefficient κ) is tested against direct numerical simulation (DNS) data. Two methods for precisely estimating the leading coefficient over any selected range of y are presented. These methods reveal that the differences between the theory and simulation are essentially within the uncertainty level of the simulation. The von Kármán coefficient physically exists owing to an approximate self-similarity in the flux of turbulent force across an internal layer hierarchy. Mathematically, this self-similarity relates to the slope and curvature of the Reynolds stress profile, or equivalently the slope and curvature of the mean vorticity profile. The theory addresses how, why and under what conditions logarithmic dependence is approximated relative to the specific mechanisms contained within the mean statement of dynamics.

1. Introduction

One may reasonably assert that the science and engineering of wall-bounded turbulent flows has been hindered by the lack of a guiding theory that is both mathematically cogent and mechanistically descriptive. This assertion largely motivates

† Email address for correspondence: joe.klewicki@unh.edu

the present authors' research to advance a first-principles-based theoretical framework that not only embraces empirically quantified behaviours but also reveals how and why these behaviours occur. The present effort explores the veracity of this theory relative to the logarithmic-like properties of the mean velocity profile, including the von Kármán constant.

The logarithmic equation for the mean velocity profile in statistically stationary turbulent wall-bounded flow is most often given by

$$\frac{U}{u_\tau} = \frac{1}{\kappa}\ln\left(\frac{yu_\tau}{\nu}\right) + B, \tag{1.1}$$

where U is mean axial velocity, u_τ is the friction velocity, ν is the kinematic viscosity, y is the distance from the wall and κ and B are constants (e.g. Tennekes & Lumley 1972; Pope 2000). Variants of (1.1) include an offset to the $y^+ = yu_\tau/\nu$ coordinate inside the logarithm (George & Castillo 1997; Oberlack 2001; Spalart, Coleman & Johnstone 2008). Logarithmic-like dependence finds considerable empirical support. Owing to this, a variety of mean profile equations, including power-law forms that are approximated by (1.1), have been constructed via a number of non-rigorous means (e.g. see Panton 2005; Buschmann & Gad-el-Hak 2007 and the references therein). Typically (1.1) is taken to be valid in some region that is simultaneously not too close and not too far from the wall. The precise validity of (1.1) and the wall-normal bounds over which it might hold are, however, largely unresolvable by approaches not grounded in first principles. This is because such approaches invariably rely upon hypotheses of a mathematical or physical nature having unknown, reasonably questionable or untestable validity (e.g. see Fife *et al.* 2009). The present approach addresses logarithmic dependence and a number of affiliated issues through an elucidation of the mathematical properties of the mean differential statement of Newton's second law.

The constant κ holds special significance in the logarithmic mean velocity equation. Effectively it represents the slope of the profile, and thus is a measure of how the turbulence distributes mean momentum as a function of y. (In the prevalent inner/outer/overlap layer-based approach to obtaining (1.1), originally formulated by Millikan (1939) and Izakson (1937), $1/\kappa$ is equal to the weighted wall-normal gradient of U under inner and outer normalization simultaneously, e.g. $1/\kappa = y^+\mathrm{d}U^+/\mathrm{d}y^+$.) The value of κ also has considerable practical importance as it appears in many engineering formulae relating to flow development and frictional drag (e.g. Schlichting & Gersten 2000). Over the years the idea that κ might be a universal constant for turbulent wall-flows has, at least in part, promoted considerable investigation into its presumably precise value. This has been primarily accomplished through increasingly careful measurements of the mean velocity profile (e.g. Zagarola & Smits 1998; Osterlund *et al.* 2000; Nagib & Chauhan 2008). Of course, empirical data can never provide positive proof for the universality of κ, or even that it is a constant. Indeed, recent experimental evidence indicates that κ varies from one wall-flow to the next (e.g. Nagib & Chauhan 2008).

The mean velocity profile is, however, a solution of the appropriately simplified Reynolds averaged Navier–Stokes equation. It is thus natural to expect κ to have a well-defined relationship to the properties of this equation. Consistent with this, detailed consideration of the mean momentum balance yields an expression for κ in terms of a scaled second derivative of the Reynolds stress (Fife *et al.* 2005*a*). The validity and ramifications of this equation are explored herein using data from direct numerical simulations (DNSs).

In what follows, the primary analytical results to be explored are first concisely presented and their nature and consequences clarified. The veracity of these analytical results are then explored using DNS data.

2. Analytical results

At the outset it is relevant to note that the present approach has been used to elucidate the behaviour of the solutions to a number of turbulent wall-flow problems, as well as to successfully reveal scaling behaviours directly from the governing equations (Wei *et al.* 2005*a,b,c*; Klewicki *et al.* 2006; Wei, Fife & Klewicki 2007; Metzger, Adams & Fife 2008). Thus, it has broader application than discussed herein.

2.1. *Momentum equation*

The analysis below is primarily for statistically stationary, fully developed, incompressible, pressure driven turbulent flow in a two-dimensional channel. The companion analysis associated with turbulent Couette flow has been presented in detail elsewhere (e.g. Fife *et al.* 2005*a*). At points throughout the presentation results from the Couette flow analyses will be cited for comparison.

The height of the channel is 2δ, x is the mean flow direction and y is normal to the channel wall. The analysis begins with the Navier–Stokes equations, which is the appropriate differential statement of Newton's second law. Applying the Reynolds decomposition, time averaging and simplifying for the given problem statement yields the x component force balance,

$$0 = -\frac{\mathrm{d}P}{\mathrm{d}x} + \mu\frac{\mathrm{d}^2U}{\mathrm{d}y^2} - \rho\frac{\mathrm{d}\langle uv\rangle}{\mathrm{d}y}, \tag{2.1}$$

where U and P denote the mean axial velocity and pressure respectively, $\langle uv\rangle$ is the time averaged correlation between the axial and wall-normal velocity fluctuations (u and v respectively), μ is the dynamic viscosity and ρ is the mass density. Neither the y nor the z components of the momentum equation enter into the analysis.

Equation (2.1) contains two unknown functions and thus is unclosed. Considerable amounts of information can, however, be ascertained regarding its solutions. Among these are the conditions for the existence of a logarithmic-like profile, including a formula for the von Kármán constant (coefficient). Results elucidated from (2.1) pertinent to these topics are now concisely presented.

The inner-normalized form of (2.1) is given by

$$0 = \frac{1}{\delta^+} + \frac{\mathrm{d}^2U^+}{\mathrm{d}y^{+2}} - \frac{\mathrm{d}\langle uv\rangle^+}{\mathrm{d}y^+}, \tag{2.2}$$

where the superscript '+' signifies normalization by the friction velocity $u_\tau = \sqrt{\tau_w/\rho}$ and kinematic viscosity $\nu = \mu/\rho$. The form of (2.2) utilized in previous publications is given by

$$0 = \epsilon^2 + \frac{\mathrm{d}^2U^+}{\mathrm{d}y^{+2}} + \frac{\mathrm{d}T^+}{\mathrm{d}y^+}, \tag{2.3}$$

where $T^+ = -\langle uv\rangle/u_\tau^2$ and $\epsilon^2 = 1/\delta^+$. Boundary conditions associated with (2.3) are $U^+ = T^+ = 0$ and $\mathrm{d}U^+/\mathrm{d}y^+ = 1$ at $y^+ = 0$, and $T^+ = \mathrm{d}U^+/\mathrm{d}y^+ = 0$ at $y^+ = 1/\epsilon^2$.

2.2. *Self-similar layer hierarchy*

Equation (2.3) admits a hierarchy of scaling layers also called patches, whose existence and properties are central elements of the analysis (Fife *et al.* 2005*a*,*b*). The hierarchy is revealed by considering the test function

$$T^{\beta}(y^{+}) = T^{+}(y^{+}) + \epsilon^{2} y^{+} - \beta y^{+}, \tag{2.4}$$

where β is a small parameter discussed further below. For the sake of clarity, it is noted that β is an identifying superscript on T^{β}, not an exponent. The choice of (2.4) may seem to be quite arbitrary. To the author's knowledge, however, it is the simplest that serves the purpose of revealing the entire hierarchy of scaling patches. Inserting the transformation (2.4) into the momentum equation (2.3) yields

$$0 = \frac{\mathrm{d}^{2} U^{+}}{\mathrm{d}y^{+2}} + \frac{\mathrm{d}T^{\beta}}{\mathrm{d}y^{+}} + \beta, \tag{2.5}$$

which is still exact.

Revealing that (2.3) formally admits a hierarchy of scaling layers draws upon the fact that for a wide range of values of β, (2.5) may be rescaled to an exact parameter invariant equation, with the rescaled variables attaining values on the patch that are also invariant. Results from the similarity analysis of differential equations indicate that parameter invariant equations with invariant boundary values yield universal solutions (e.g. Hansen 1964; Cantwell 2002). This property of well-posed differential equation problems does not always hold for the turbulent wall-flow equation (2.4) because it is underdetermined (one equation with two unknowns). Nevertheless, the similarity properties of this equation under various scalings point to solutions that are universal in order of magnitude. A complication is the fact that the dominant terms in the equation change with distance from the wall in ways that, in general, are not *a priori* known (Fife *et al.* 2005*b*; Wei *et al.* 2005*a*). This reality factors significantly since it necessitates a rescaling in order to construct a parameter free invariant equation.

For a range of β, T^{β} will exhibit a single local maximum at a position y_m^{β} somewhere in the flow domain. This is known from the boundary conditions on T^{+}. As each admissible y_m^{β} is approached from below there is seen to be a scaling, depending on β, and a corresponding layer L_{β}, nominally centred on y_m^{β} within which all three terms in (2.5) are of the same formal order of magnitude. This also occurs relative to (2.2) as T^{+} approaches its peak, and is associated with a balance breaking and exchange of mean forces having significant physical implications (Wei *et al.* 2005*a*; Klewicki *et al.* 2007). The required rescaling is most easily accomplished using differential transformations. While more general differential transformations reveal the full extent of possibilities (Fife, Klewicki & Wei 2009), the simplest yielding the basic scaling behaviour of the layer hierarchy is given by

$$\mathrm{d}y^{+} = \beta^{-1/2}\mathrm{d}\hat{y}, \qquad \mathrm{d}T^{\beta} = \beta^{1/2}\mathrm{d}\hat{T}^{\beta}. \tag{2.6}$$

Subsequently applying this transformation to (2.5) yields the desired parameter-free invariant equation,

$$0 = \frac{\mathrm{d}^{2} U^{+}}{\mathrm{d}\hat{y}^{2}} + \frac{\mathrm{d}\hat{T}^{\beta}}{\mathrm{d}\hat{y}} + 1, \tag{2.7}$$

for each value of β in its admissible range (Fife *et al.* 2005*a*,*b*). No approximation is used in deriving (2.7); it is exact. Moreover the three terms in (2.7) can be evaluated

at the location $y^+ = y_m^\beta$, i.e. $\hat{y} = 0$, and shown to be parameter independent and $O(1)$ in magnitude (specifically $-1, 0, 1$). These terms have the same order of magnitude in a neighbourhood of $\hat{y} = 0$ as well. This is strong evidence that the transformation (2.6) provides a scaling layer containing that point, and that there is an order of magnitude invariance of the solutions $U^+(\hat{y})$ and $\hat{T}^\beta$ as one passes from one such layer to another, i.e. as β varies. In this regard, note that the width of each L_β can only be determined to order of magnitude. The values of the terms in (2.7) on the periphery of each L_β are also revealed to be invariant when these positions on the periphery are consistently located a characteristic length, $\hat{y} = O(1)$, from the patch centre, $\hat{y} = 0$ (Fife *et al.* 2005*b*; Wei *et al.* 2005*a*; Fife *et al.* 2009).

Given the second relation in (2.6) and the fact that at each y_m^β,

$$\beta = \frac{\mathrm{d}T^\beta}{\mathrm{d}y^+} = \frac{\mathrm{d}T^+}{\mathrm{d}y^+} + \epsilon^2, \tag{2.8}$$

it can be shown that the width of each L_β layer is

$$W(y^+) = O(\beta^{-1/2}), \tag{2.9}$$

and that these layer widths asymptotically scale with the distance from the wall, y (Fife *et al.* 2005*a*,*b*). This attribute of the scale hierarchy has mathematical and physical significance as it provides a fundamental reason for the *distance from the wall* length scale inherent to turbulent wall-flows that is often assumed in scaling arguments and long associated with logarithmic dependence. Its also resembles many of the features assumed in the attached eddy hypothesis of Townsend (1976), and embodied in the associated models of Perry & Chong (1982) and Perry & Marusic (1995).

Since there is a continuum of layers, parameterized by β, the question arises as to what happens in the intersection of two layers. This is made clearer by recognizing that the solution in L_β depends on both β and ϵ, and the asymptotics are with respect to both parameters approaching 0. Let us simply consider the case that the two parameters are connected by a power law, $\beta = \epsilon^b$, so that b is the new parameter in place of β. Suppose the two layers in question correspond to parameters β_1 and $\beta_2 > \beta_1$. They have widths of the orders $W_1 = \epsilon^{-b_1/2}$ and $W_2 = \epsilon^{-b_2/2}$. The ratio is $W_1/W_2 = \epsilon^{(b_2-b_1)/2}$. Fix the bs and let $\epsilon \to 0$. The ratio also approaches 0, so that for small enough ϵ, there is no more overlap. If ϵ is small but not that small, there will be an overlapping region where both scalings can be used to represent approximate solutions. In any case, within a given L_β, the approximation constructed for that layer will become less accurate as one moves away from the centre point y_m^β. This is reminiscent of aspects of Taylor series expansions, but is actually quite different.

Relation (2.8) reveals that the L_β depend directly upon the properties of the Reynolds stress gradient. In particular, the decay rate of this gradient establishes the admissible range of β values, as well as the corresponding range of y^+ values over which the hierarchy exists. As depicted in figure 1 this latter range is given by $30 \lesssim y^+$, $y/\delta \lesssim 0.5$ (Fife *et al.* 2005*b*). At the upper end of this range the layer thickness (characteristic length) is maximal. For future reference, the bounds of the layer hierarchy are also depicted in figure 2. This figure plots the function $y^+ \mathrm{d}U^+/\mathrm{d}y^+$ that is often used in exploring issues associated with logarithmic dependence. The data in this figure are from the channel flow simulation of Hoyas & Jimenez (2006) at $\delta^+ = 547, 934$ and 2003. Figure 2 reveals that the upper and lower boundaries of the hierarchy bracket the region typically associated with logarithmic dependence, and

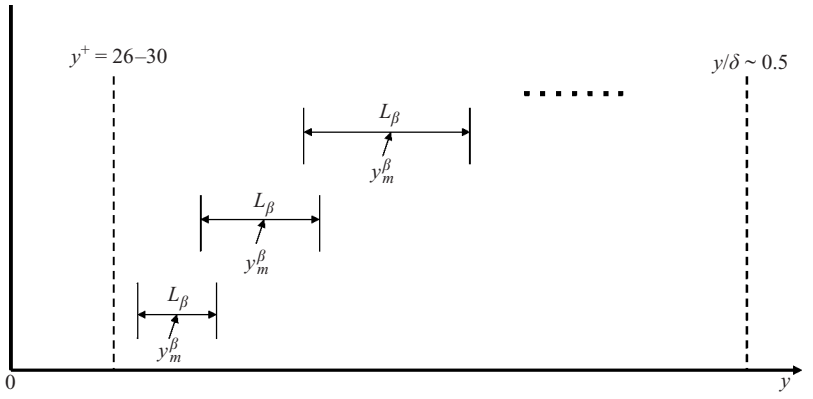

FIGURE 1. Schematic depiction of the continuum of scaling layers formally admitted by the mean momentum equation. Note that the invariant form (2.7) is valid on each L_β.

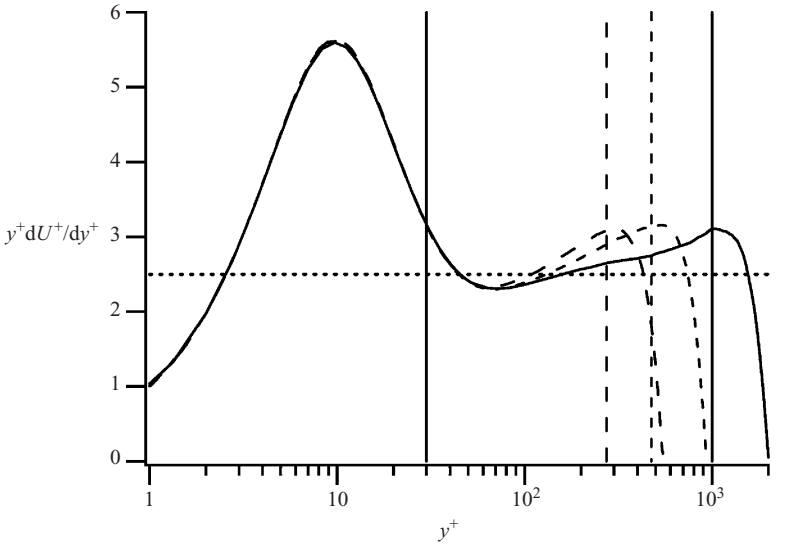

FIGURE 2. Mean velocity profile slope indicator function $y^+ dU^+/dy^+$ as computed from the data of Hoyas & Jimenez (2006): $\delta^+ = 547$, – – –; $\delta^+ = 934$, - - - -; $\delta^+ = 2003$, ——. Vertical lines denote the ranges of the layer hierarchy. The horizontal line is at 2.5, corresponding to $\kappa = 0.4$.

that the upper boundary tracks the position where the diagnostic function drops-off precipitously. If, for a range of y^+, there exists an exactly logarithmic mean velocity profile this indicator function attains a constant value equal to $1/\kappa$. For comparison, a constant line at $1/\kappa = 2.5$ ($\kappa = 0.4$) is also shown.

Figure 3 presents the inner normalized Reynolds stress gradient profiles for Couette and channel flow. These functions are highly similar, as is the profile of dT^+/dy^+ for the zero pressure gradient boundary layer (e.g. see figure 4 of Fife *et al.* 2005*b*). Closer examination of these profiles in figure 4, however, reveals differences in the region typically associated with logarithmic variation in the mean profile. The present theory indicates that properties associated with the slope and curvature of the Reynolds stress profile underlie logarithmic-like behaviour. The subtle differences between the dT^+/dy^+ profiles account for the observed differences in the mean profiles of turbulent

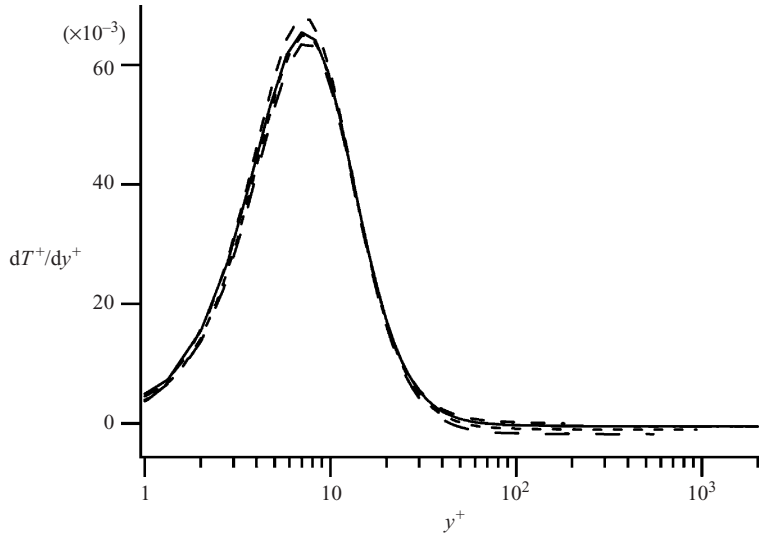

FIGURE 3. Profiles of the Reynolds stress gradient $\mathrm{d}T^+/\mathrm{d}y^+$ from channel and Couette flow. Channel flow data are from Hoyas & Jimenez (2006): $\delta^+ = 547$, ————; $\delta^+ = 934$, - - -; $\delta^+ = 2003$, ——. Couette flow data are from Kawamura, Abe & Shingai (2000): $\delta^+ = 180$, – – –.

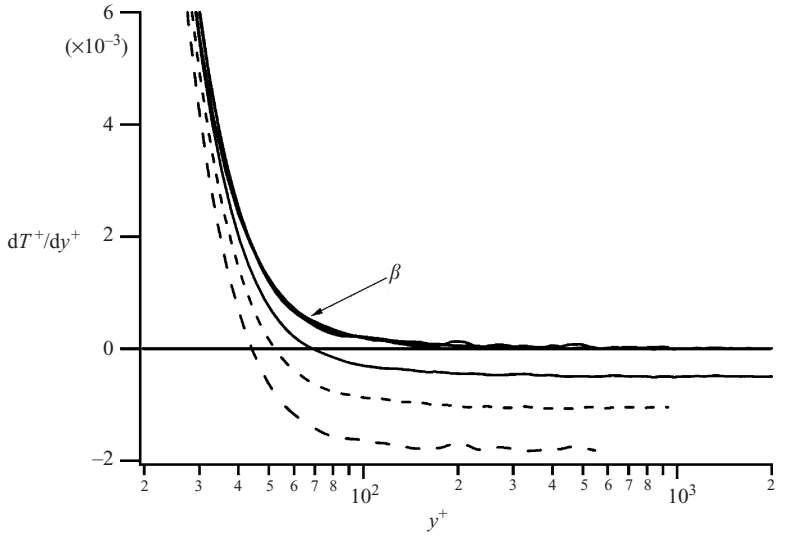

FIGURE 4. Expanded view of the $\mathrm{d}T^+/\mathrm{d}y^+$ profiles of figure 3. Profiles of $\beta = \mathrm{d}T^+/\mathrm{d}y^+ + \epsilon^2$ for each channel flow follow the same profile as $\mathrm{d}T^+/\mathrm{d}y^+$ in Couette flow.

wall-flows as well as provide insight regarding important dynamical processes (Fife *et al.* 2005*b*; Klewicki *et al.* 2007). For example, the zero crossings in the channel flow profiles reflect the position of the Reynolds stress maximum y_m^+, which signifies the transition from a force balance dominated by the viscous and Reynolds stress gradients to one dominated by the pressure gradient and Reynolds stress gradient in (2.3). This has relevance to figure 4 in that at each y_m^β, $\beta = \mathrm{d}T^+/\mathrm{d}y^+ + \epsilon^2$ in channel flow, while in Couette flow at each y_m^β, $\beta = \mathrm{d}T^+/\mathrm{d}y^+$. Thus the differences between the channel flow $\mathrm{d}T^+/\mathrm{d}y^+$ profiles and the Couette flow $\mathrm{d}T^+/\mathrm{d}y^+$ profile effectively equals

ϵ^2, and the β profiles as given by (2.8) are invariant to within less than the magnitude of β at the large scale end of the hierarchy (i.e. smaller in order of magnitude than the minimal value of β on the hierarchy). This analytical finding relating Couette and channel flow is embodied in the invariance of the β curves in figure 4. Regarding this comparison it is also relevant to note that the mean dynamics in Couette flow are everywhere described by a balance between the viscous and Reynolds stress gradients, while in channel flow they are described by the four layer structure given in Wei *et al.* (2005*a*) of which layer II is described by a balance between the Reynolds and viscous stress gradients. Thus, δ^+ for Couette flow in many respects corresponds to the layer II thickness in a channel flow, only at a much higher effective Reynolds number.

2.3. *Logarithmic dependence*

Properties associated with a logarithmic mean velocity profile follow directly from the attributes of the layer hierarchy. Most prominent among these are that the mean statement of dynamics can be written in an invariant form when normalized by the appropriate local characteristic length of the hierarchy (2.7), and that the characteristic widths of the L_β scale according to (2.9). One consequence of these is that at each y_m^β ($\hat{y}=0$) on the hierarchy the locally normalized curvature of the locally normalized Reynolds stress becomes an $O(1)$ quantity (Fife *et al.* 2005*a*,*b*),

$$A(\beta) = -\frac{\mathrm{d}^2\hat{T}^\beta}{\mathrm{d}\hat{y}^2}(0). \tag{2.10}$$

Since the hierarchy constitutes a continuum of layers, there is in fact a y_m^β at each y^+ within the admissible range. Furthermore, relative to the computation of $A(\beta)$ it will prove useful to employ the alternative expressions,

$$\frac{\mathrm{d}^2\hat{T}^\beta}{\mathrm{d}\hat{y}^2} = \beta^{-3/2}\frac{\mathrm{d}^2T^+}{\mathrm{d}y^{2+}} = \frac{\mathrm{d}^2T^+}{\mathrm{d}y^{2+}}\left(\frac{\mathrm{d}T^+}{\mathrm{d}y^+}+\epsilon^2\right)^{-3/2} \tag{2.11}$$

and

$$\frac{\mathrm{d}^2\hat{T}^\beta}{\mathrm{d}\hat{y}^2} = \beta^{-3/2}\frac{\mathrm{d}^2T^+}{\mathrm{d}y^{2+}} = \frac{\mathrm{d}^2T^+}{\mathrm{d}y^{2+}}\left(\frac{\mathrm{d}T^+}{\mathrm{d}y^+}\right)^{-3/2} \tag{2.12}$$

for channel and Couette flow respectively. Other alternative but equally valid expressions will be presented later.

The invariance of (2.7) and the individual terms in this equation at the periphery of the L_β centred on each y_m^β (see figure 1) supports the assertion that $A(\beta)$ may attain approximately constant values over an interior subrange of L_β (Fife *et al.* 2005*b*). Note that this is not an assumption, but simply a possibility. The degree to which A attains constancy directly reflects the degree of self-similarity from one L_β to the next. That is, if A is exactly equal to a constant over some range of y, then across the hierarchy of layers corresponding to that range of y there is exact self-similarity. By considering the variation of y_m^β with β one may employ the definition of β and the once integrated form of the momentum equation to derive differential equations for the Reynolds stress profile and mean velocity profile (on the hierarchy) that contain the $O(1)$ quantity, A (Fife *et al.* 2005*a*,*b*; 2009). Under the condition that A equals a constant (exactly or approximately), these expressions may be integrated and thus analytically connect (2.3) to an equation for the mean profile. Specifically, the mean profile expression on the layer hierarchy for both planar Poiseuille and Couette flow is found to be

$$U^+(y^+) = (2/A)^2\ln(y^+ - C) + D. \tag{2.13}$$

In (2.13) A is the $O(1)$ function $A(\beta)$ given by (2.10) and C and D are constants (Fife *et al.* 2005*a*). If A is not exactly constant, then the resulting mean equation is bounded above and below by logarithmic functions having the same form as (2.13) (Fife *et al.* 2005*a*). Note that the logarithmic formula found from the mean momentum equation yields an offset in the argument of the logarithm. This fact has bearing on those studies that have recently investigated this issue (e.g. Spalart, Coleman & Johnstone 2008). Note also that (2.13) provides a definition for the leading coefficient that is free of any adjustable constants. This equation reveals that the observation of logarithmic-like behaviour is associated with the degree to which dynamical self-similarity (necessarily approximate) is attained from one layer to the next on the L_β hierarchy. Comparison of (2.13) to (1.1) yields an independent definition for κ,

$$\kappa = \frac{A^2}{4} = \frac{1}{4}\left[\frac{\mathrm{d}^2T^+}{\mathrm{d}y^{+2}}\beta^{-3/2}\right]^2 = \frac{1}{4}\left[\frac{\mathrm{d}^2T^+}{\mathrm{d}y^{+2}}\left(\frac{\mathrm{d}T^+}{\mathrm{d}y^+}+\epsilon^2\right)^{-3/2}\right]^2, \tag{2.14}$$

and thus the constancy of the function κ is a direct measure of how closely exact self-similarity is attained.

Equivalent forms for κ are available. These are useful for the purposes of computing quantities from discrete data. By virtue of (2.3),

$$\beta = -\frac{\mathrm{d}^2U^+}{\mathrm{d}y^{+2}}, \tag{2.15}$$

and thus,

$$\kappa = \frac{1}{4}\left[\frac{\mathrm{d}^2T^+}{\mathrm{d}y^{+2}}\left(-\frac{\mathrm{d}^2U^+}{\mathrm{d}y^{+2}}\right)^{-3/2}\right]^2. \tag{2.16}$$

Similarly, consideration of the mean vorticity transport equation

$$0 = \frac{\mathrm{d}^2\Omega_z^+}{\mathrm{d}y^{+2}} + \frac{\mathrm{d}^2T^+}{\mathrm{d}y^{+2}}, \tag{2.17}$$

where $\Omega_z^+ = -\mathrm{d}U^+/\mathrm{d}y^+$, yields

$$\kappa = \frac{1}{4}\left[\left(-\frac{\mathrm{d}^2\Omega^+}{\mathrm{d}y^{+2}}\right)\left(-\frac{\mathrm{d}^2U^+}{\mathrm{d}y^{+2}}\right)^{-3/2}\right]^2 = \frac{1}{4}\left[\frac{\mathrm{d}^3U^+}{\mathrm{d}y^{+3}}\left(-\frac{\mathrm{d}^2U^+}{\mathrm{d}y^{+2}}\right)^{-3/2}\right]^2. \tag{2.18}$$

This last form will prove to give the lowest uncertainty in quantities computed from data. This form is also physically intriguing as it speaks to the self-similarity in the simultaneous processes of wallward momentum transport and wall-normal vorticity transport (Klewicki *et al.* 2007; Eyink 2008).

Equations (2.9), (2.10), (2.13), (2.14), (2.16) and (2.18) directly arise solely through consideration of (2.1).

3. Comparing theory and data

This section explores the analytical findings outlined above. Primary concerns are the predicted properties of the layer hierarchy and the affiliated behaviours associated with logarithmic dependence. The latter of these includes validation of the theory at at least two increasingly stringent levels. The first relates to whether $A(\beta)$ is indeed $O(1)$ within the analytically predicted bounds of the L_β hierarchy. The second relates to whether the data provide support for the specific prediction $A^2/4 \simeq 0.4$, i.e. (2.14)

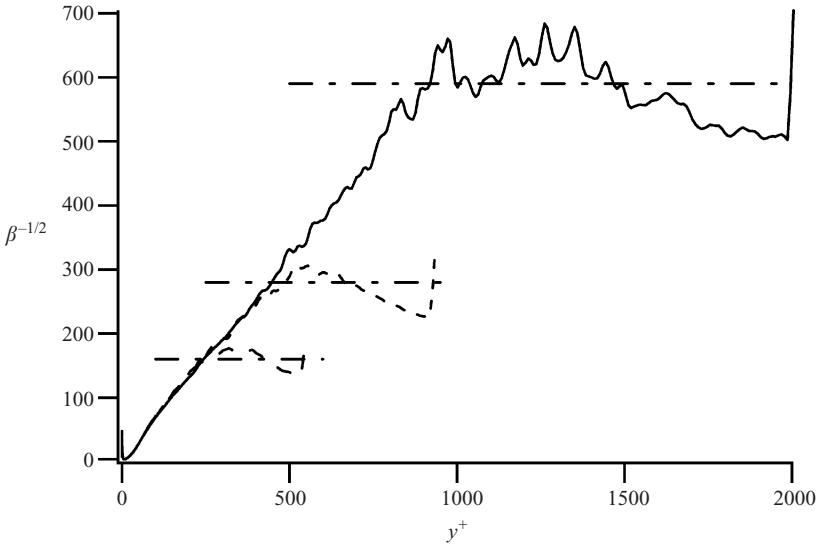

FIGURE 5. Characteristic lengths of the continuum of scaling layers in turbulent channel flow as a function of y^+, $\delta^+ = 547$, ———; $\delta^+ = 934$, – – –; $\delta^+ = 2003$, ——. Horizontal lines, —·—·—, denote approximate point at which $\beta^{-1/2}$ deviates from a linear y dependence.

holds on a subdomain interior to the bounds of the L_β hierarchy. Consistent with the aims stated at the outset, data comparisons focus on understanding the nature of the solutions to (2.1) and the affiliated physical implications.

3.1. *Layer hierarchy*

The principal elements relating to the layer hierarchy as predicted by the theory pertain to (i) the existence of a parameter free invariant form of the momentum equation on each L_β, and (ii) the existence of the predicted characteristic length scale distribution associated with the width of each L_β. The former of these is strictly a matter of analysis, and has been established. Thus, we focus attention on the latter.

The essential features of the L_β are that they exhibit a linear dependence with distance from the wall (increasingly so as $\delta^+ \to \infty$), they exhibit this dependence interior to $y^+ \simeq 30$ and $y/\delta \simeq 0.5$, and because of this the maximum characteristic length associated with the hierarchy occurs near $y/\delta = 0.5$. The continuous distribution of the characteristic widths of the L_β (2.9) are plotted across the entire channel half-width in figure 5 for the three channel flow Reynolds numbers of Hoyas & Jimenez (2006). As is clear, the characteristic lengths exhibit a linear variation with distance from the wall. Furthermore, each of the curves break from this linear trend in the range $0.45 \lesssim y/\delta \lesssim 0.5$. In each case, the maximal length (occurring at the end of the hierarchy) is about $\delta/3$. Interestingly, for $y/\delta > 0.5$ the length scale function attains a peak value and then drops below the peak value on the linear curve at about $y/\delta = 0.75$. This is made apparent by the variations about the horizontal lines on the figure.

Figure 6 shows a close-up of the three channel flow profiles along with the Couette flow profile of Kawamura *et al.* (2000). The four profiles convincingly merge to a single profile for $y^+ < 120$. Furthermore, in good agreement with the analytical prediction these profiles begin to exhibit a linear-like trend for y^+ greater than about 30. Interestingly, for $30 \lesssim y^+ \lesssim 100$ the slope of this part of the length scale profile

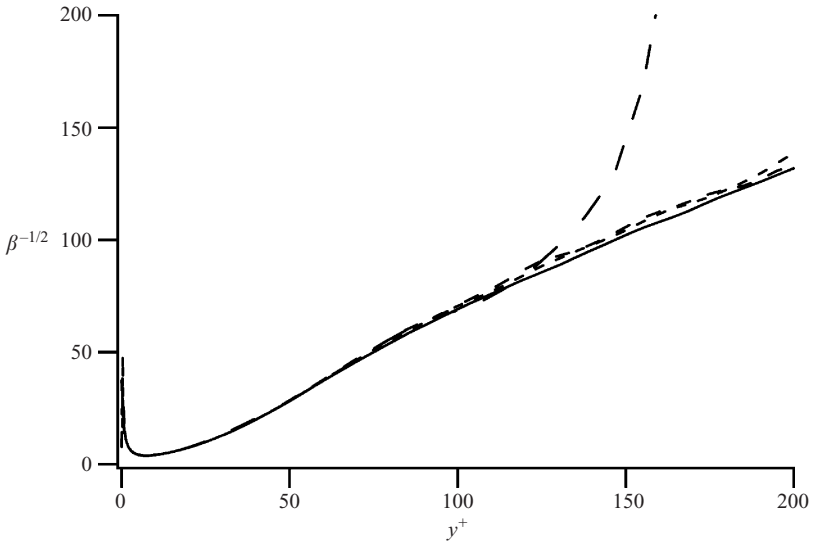

FIGURE 6. Characteristic lengths of the continuum of scaling layers in the vicinity of the wall in turbulent channel flows $\delta^+ = 547$, ———; $\delta^+ = 934$, – – –; $\delta^+ = 2003$, —— (Hoyas & Jimenez 2006) and turbulent Couette flow $\delta^+ = 180$, — - — - — (Kawamura *et al.* 2000).

is steeper than for $y^+ > 100$. According to the theory, any linear dependence in the length scale will lead to logarithmic-like behaviour in the mean profile, but a changing length scale slope may trigger a change in the logarithmic slope of the mean profile. The data of figure 2 clearly reveal that this is the case, as do the estimates for the coefficient $A(\beta)$ below. Previous studies provide evidence that the logarithmic mean profile has a different slope for $y^+ < y_m^+$ than for $y^+ > y_m^+$ (Afzal 1982; Osterlund *et al.* 2000). In the context of the present theoretical framework, this has to do with the aforementioned fact that the mean force balance changes from one dominated by the viscous and Reynolds stress gradients to one dominated by the Reynolds stress and pressure gradients. The Couette flow profile in figure 6 reveals that the upper boundary of the hierarchy is at about $y^+ = 120$. This corresponds to a length of about 80, and thus the maximal length in Couette flow appears to be about 0.44δ, which is larger than observed in figure 5 for channel flow. The analysis of Fife *et al.* (2005*b*) estimates that the maximal L_β for Couette flow extends to within about 12 % of δ from the centreline. Nominally, centring a layer having a width of $\Delta y^+ = 80$ at $y^+ = 120$ puts the upper boundary at $y^+ \simeq 160$, or within about 11 % from $y^+ = \delta^+ = 180$.

The analytical findings of Fife *et al.* (2005*b*) indicate that the hierarchy will end when β drops to an order of magnitude much smaller than $(\mathrm{d}T^+/\mathrm{d}y^+)_{max}/10$ but greater than $O(\epsilon^4)$. The channel flow simulation data of Hoyas & Jimenez (2006) confirm this result as the minimum β on the hierarchy (i.e. at $y/\delta = 0.5$) is given by about $12\epsilon^4$ at all three Reynolds numbers.

3.2. *Logarithmic dependence and* κ

The above data bear out the veracity of the analytical results that predict the existence and properties of the L_β hierarchy. Given these properties, the continuous rescaling of (2.3) that leads to the parameter free invariant form (2.7) on each L_β establishes that $A(\beta)$ is $O(1)$. It is a relatively simple matter to show that the range of possible

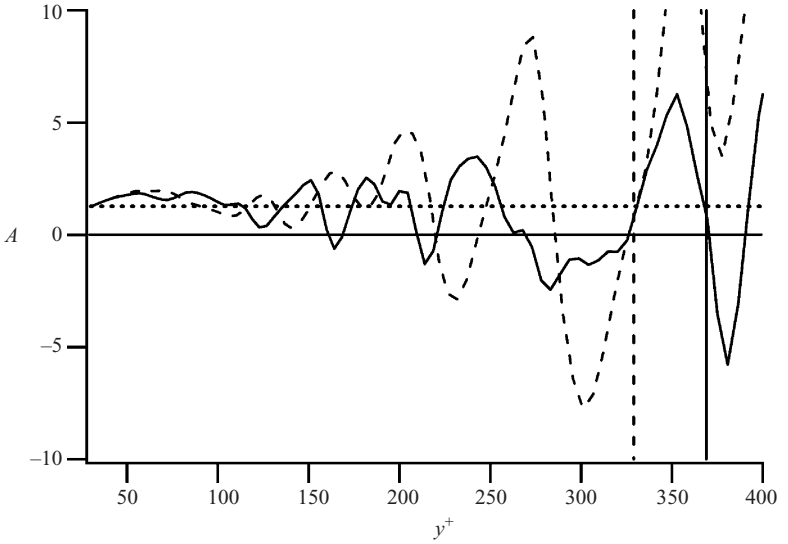

FIGURE 7. Leading coefficient $A(\beta)$ in logarithmic mean profile equation (2.13) as computed using method 1 (2.14) from the $\delta^+ = 2003$, ——; and $\delta^+ = 934$, – – – data of Hoyas & Jimenez (2006). Dotted line is at $A = 1.265$ corresponding to $\kappa = 0.40$.

characteristic lengths on the L_β hierarchy increases with increasing δ^+ (Fife *et al.* 2005*a*). From this, and the fact that $\beta^{-1/2}$ becomes an increasingly linear function as $\delta^+ \to \infty$, one expects that for sufficiently high δ^+ $A(\beta)$ will become approximately constant on an interior domain of the hierarchy, and that it will better approximate a constant as $\delta^+ \to \infty$. Even if this were not true, however, (2.13) still holds if A is a constant, and if A is approximately constant the resulting mean profile equation is bounded by logarithmic functions having the same form as (2.13).

It is appropriate to describe results for both the approximate and exact cases for at least two reasons. The first is that from measurements one can only confirm that the mean profile is logarithmic-like. The second and more substantive reason is that analyses of the mean momentum equation (summarized in § 2) reveal that A is explicitly a measure of the self-similarity of dynamical processes across some range of L_β. Thus, for example, imperfections in the boundary conditions, the non-constancy of mean advection in boundary layer flow, or external influences on the hierarchy owing to finite δ^+ will essentially always result in approximate self-similarity from one L_β to the next. As noted previously, approximate self-similarly generically means that A will only be approximately constant.

By virtue of the first equality in (2.14) what is true about the constancy (or non-constancy) of A is also true about κ. The data presentation below supports the assertion that A is approximately constant ($\simeq 0.4$) in an interior zone of the hierarchy where logarithmic-like dependence is typically observed, and provides evidence that the leading coefficient, traditionally expressed as the von Kármán constant, equals $A^2/4$.

We begin by demonstrating that computations of A that employ the direct use of (2.14), (2.16) or (2.18) exhibit considerable uncertainty. This is because these computations involve taking the ratio of higher order derivative quantities that are also becoming decreasingly small with increasing y^+. For example, figure 7 presents the distributions of A in the region $30 < y^+ < 400$ for the two highest channel flow

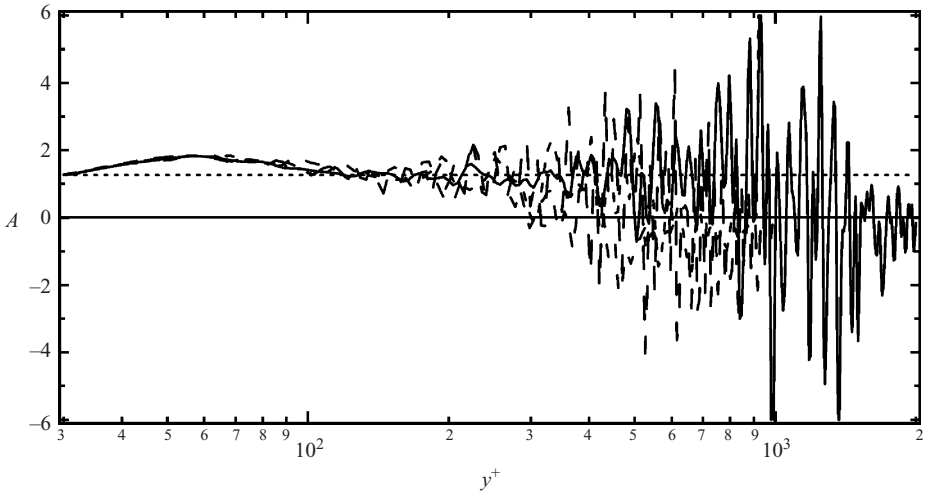

FIGURE 8. Leading coefficient $A(\beta)$ in logarithmic mean profile equation (2.13) as computed using method 3 (2.18) from the $\delta^+ = 2003$, —; and $\delta^+ = 934$, - - - data of Hoyas & Jimenez (2006) and the $\delta^+ = 1016$, – – –; and $\delta^+ = 636$, — — — data of Kawamura *et al.* (2000). Dotted line is at $A = 1.265$ corresponding to $\kappa = 0.40$.

Reynolds numbers of Hoyas & Jimenez (2006) computed using (2.14). This equation purely employs the derivatives of T^+, which are expected to be noisier than those of U^+. These data are well behaved near the wall, and then begin to oscillate about a non-zero mean. As indicated by the horizontal dotted line, this non-zero mean appears to be close to $\kappa = A^2/4 = 0.4$ ($A = 1.265$). In the region $30 \lesssim y^+ \lesssim 100$, the data of figure 7 attains an approximately constant value that lies above the $\kappa = 0.4$ line. This is in accord with the observed change in the slope of the characteristic length distribution as noted relative to figure 6, and confirmed by the logarithmic indicator function of figure 2. For $y^+ > 100$ the excursions are increasingly large and infrequent. A rough estimate of the average value of A can be obtained by considering an even number of positive and negative oscillations. Estimates obtained by averaging between the start of the hierarchy ($y^+ \simeq 30$) and the indicated vertical lines for $\delta^+ = 934$ and $\delta^+ = 2003$ yield $A = 1.296$ ($\kappa \simeq 0.42$) and $A = 1.234$ ($\kappa \simeq 0.38$), respectively. Owing to the obviously high uncertainties it is emphasized that these values are only viewed as rough estimates. Note also that the indicator functions in figure 2 clearly reveal that the slope noticeably varies in the region generally attributed to logarithmic behaviour, i.e. the profile slope is a slowly varying function. In fact, however, the present theory indicates that this is essentially always the case. The leading coefficient is never expected to be exactly a constant, but only better approximate constancy as $\delta^+ \to \infty$. The channel flow results of Kawamura *et al.* (2000) (at $\delta^+ = 636$ and 1016) and those of Moser, Kim & Mansour (1999) (at $\delta^+ = 587$), with derivatives computed using the Chebychev polynomial method employed in the original DNS, have also been tested but are not shown. These exhibit essentially identical results to those displayed in figure 7. Estimates of A using (2.16) exhibit results that are also similar to those shown in figure 7.

Since it only employs derivatives of the mean velocity, computations using (2.18) are expected to be more well behaved than those using (2.14) or (2.16). Figure 8 reveals that this is indeed the case. In this figure the region $30 \lesssim y^+ \lesssim 100$ is shown to be one of continuously varying A corresponding to the continuously varying curve

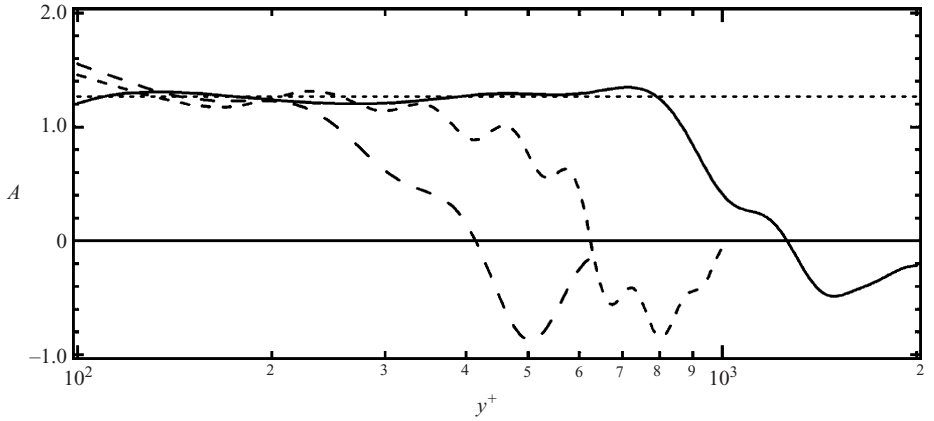

FIGURE 9. Smoothed $\delta^+ = 636$, 1016 and 2003 profiles of figure 8. Dotted line is at $A = 1.265$ corresponding to $\kappa = 0.40$.

in figure 2 over the same y^+ range. A conventional average over the entire domain of each L_β hierarchy yields $A = 1.303$ ($\kappa \simeq 0.42$) at $\delta^+ = 636$, $A = 1.230$ ($\kappa \simeq 0.38$) at $\delta^+ = 947$, $A = 1.285$ ($\kappa \simeq 0.41$) at $\delta^+ = 1016$ and $A = 1.266$ ($\kappa \simeq 0.4$) at $\delta^+ = 2003$. The data of figure 8 also verify that the behaviour of A and its relation to κ is strictly confined to the L_β hierarchy. That is, as the hierarchy is exited near $y/\delta = 0.5$ figure 8 indicates that the curves transition from fluctuating about $A = 1.265$ ($\kappa = 0.4$) to fluctuating about $A \simeq 0$. This transition at the large scale end of the hierarchy is more clearly demonstrated in figure 9, which was obtained by repeatedly applying a Savitzky–Golay smoother to the $\delta^+ = 636$, 1016 and 2003 data.

Overall, the estimates derived from figures 7 and 8 exhibit considerable uncertainty. Even so, they are consistent with the theoretical predictions that over an interior domain A is bounded and that $A^2/4 \simeq 0.4$. These figures also reveal that the detailed exploration of the present theory will have to rely on other, less sensitive, computations.

3.3. *More precise estimates of the leading coefficient*

Thus far the data presentation provides substantive support for all of the theoretical predictions outlined in §2 regarding the existence and nature of logarithmic dependence. In this regard, an inherent and overarching notion is that this leading coefficient $A^2/4$ is not a constant, but rather an $O(1)$ quantity that may attain approximate constancy on the L_β hierarchy depending on whether a specific type of dynamical self-similarity is obtained from one L_β to the next. Relative to the aims articulated at the outset, this constitutes a precise elucidation, within the context of the relevant dynamical mechanisms, of how, why and under what conditions logarithmic-like dependence occurs. Overall, one may reason that the answers to such questions are both intellectually more interesting and scientifically more important than the precise value of this coefficient κ that is often taken to be a constant.

Largely owing to technological applications there has been considerable interest within the wall-turbulence community in computing the precise value of κ over a given y^+ range. Of course, such computations implicitly operate under the supposition that κ is indeed a constant, while the present analyses reveal that this supposition only constitutes a theoretical ideal. The theory does indicate, however, that with increasing

Reynolds number variations in the leading coefficient will become increasingly difficult to discern experimentally.

We now obtain better estimates for the value of κ under the assumption that it behaves like a constant over some y^+ range. Unlike previous approaches to determining κ, the methods below utilize independent theoretical predictions. In this context, it is worth reiterating that the data in figure 2 show that for the given Reynolds numbers the slope of the mean profile noticeably varies in the region typically identified with logarithmic-like behaviour. For any computation that seeks to assign a single (average) value to κ over some y^+ range (y_1^+, y_2^+) this single value must fall between the minimum and maximum values of $(y^+ \mathrm{d}U^+/\mathrm{d}y^+)^{-1}$ between y_1^+ and y_2^+. Below we validate to this level of uncertainty. In this regard, it is also worth noting that the veracity of the present theory is the only apparent reason to expect that the present estimates should fall between these bounds, or for that matter even behave anything like a constant.

3.3.1. *Effective derivative method*

As just mentioned, $\kappa = A^2/4$ owing to a specific type of self-similarity. This self-similarity is reflected by (2.10) rewritten as

$$A\beta^{3/2} = -\frac{\mathrm{d}^2 T^+}{\mathrm{d}y^{+2}} \tag{3.1}$$

or in terms of velocity derivatives

$$A\left(-\frac{\mathrm{d}^2 U^+}{\mathrm{d}y^{+2}}\right)^{3/2} = \frac{\mathrm{d}^3 U^+}{\mathrm{d}y^{+3}}. \tag{3.2}$$

Now if one supposes that κ is truly constant, then so is A, and one may define an effective third derivative

$$\left(\frac{\mathrm{d}^3 U^+}{\mathrm{d}y^{+3}}\right)_e = \sqrt{4\kappa}\left(-\frac{\mathrm{d}^2 U^+}{\mathrm{d}y^{+2}}\right)^{3/2}. \tag{3.3}$$

Equation (3.3) provides the basis for an error minimization process to determine the *optimal* value of κ. Namely, κ is adjusted until the average absolute difference,

$$\langle \Delta \rangle = \left\langle \left| \left(\frac{\mathrm{d}^3 U^+}{\mathrm{d}y^{+3}}\right) - \left(\frac{\mathrm{d}^3 U^+}{\mathrm{d}y^{+3}}\right)_e \right| \right\rangle, \tag{3.4}$$

is minimized over some y^+ range. In this way, minimizing the average deviation from the theoretical ideal is used to estimate κ. Of course, it should be noted that this method requires reliable measurements of higher order velocity derivatives. This presents a formidable experimental challenge, and at present essentially restricts the method to employing DNS data.

Figure 10 graphically depicts the results of this process over the range $120 \leqslant y^+ \leqslant 400$. The absolute value of the difference between $\left(\mathrm{d}^3 U^+/\mathrm{d}y^{+3}\right)_e$ and $\mathrm{d}^3 U^+/\mathrm{d}y^{+3}$ as a function of y^+ is also presented. It is relevant to note that the ratio of this difference to the value of $\mathrm{d}^3 U^+/\mathrm{d}y^{+3}$ ranges between 0.1 and 0.01, and thus the effective signal-to-noise ratio is quite large. By varying κ the minimum average difference over the given y^+ range is found to be 4.45×10^{-8}, and the associated estimate for κ is 0.379. No special significance is attributed to this precise value owing to the fact that in reality the leading coefficient is not exactly constant. Note that this assertion is independent of the fact that the analysis employs relatively low Reynolds

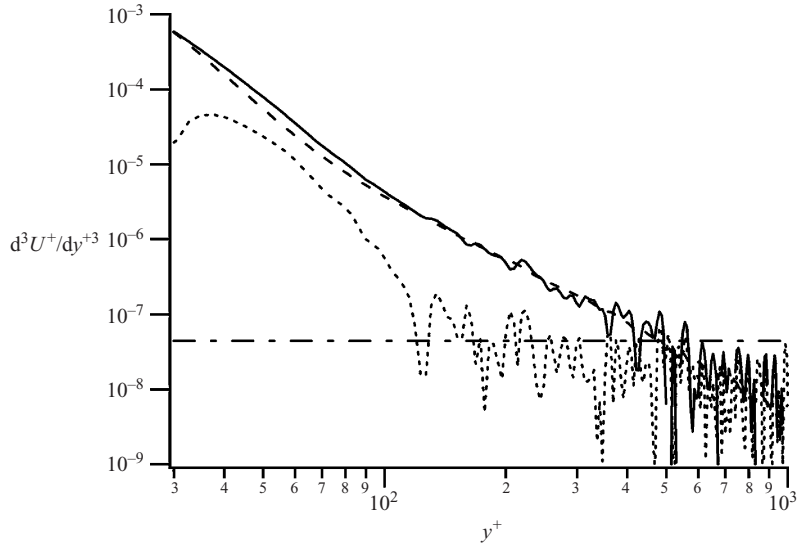

FIGURE 10. d^3U^+/dy^{+3} profiles as computed directly from the $\delta^+ = 2003$ simulation results of Hoyas & Jimenez (2006), —; and using the profile of d^2U^+/dy^{+2} from the same DNS and (3.3), - - -. The optimal value of $A = 1.232$ ($\kappa = 0.379$) minimizes the absolute value of the difference $\Delta = |(d^3U^+/dy^{+3}) - (d^3U^+/dy^{+3})_e|$ averaged over the specified range $120 \leqslant y^+ \leqslant 400$, $\Delta(y^+)$, ...; $\langle\Delta\rangle = 4.45 \times 10^{-8}$, — - — - —.

number data. Rather, it is based upon the analytical prediction of the theory indicating that over an internal domain the leading coefficient will asymptotically approximate a constant. Thus, at any δ^+ one should expect to obtain a slightly different value for κ if the average is computed over a different range of L_β. For comparison, over the same y^+ interval the $\delta^+ = 2003$ indicator function in figure 2 ranges between 2.41 and 2.71 (corresponding to $0.369 \leqslant \kappa \leqslant 0.415$) with an average value of 0.384. If one is interested in associating κ with inertially dominated flow, then the y^+ range selected should be outside layer III as prescribed by Wei *et al.* (2005*a*), i.e. over a range of y^+ values on the hierarchy for $y^+ \gtrsim 2.6\sqrt{\delta^+}$. Indeed, close examination of figure 2 reveals that the $\delta^+ = 547$ and 934 curves break from the $\delta^+ = 2003$ curve very near $y^+ = 2.6\sqrt{\delta^+}$.

The data presentation of figure 10 also makes a statement about the veracity of the theory as reflected by (2.10) and how this similarity statement analytically connects the governing differential equation (2.2) to its solution for the mean profile (2.13). Succinctly, over the range $120 \leqslant y^+ \leqslant 400$, the present theory agrees with the DNS profile of d^3U^+/dy^{+3} to within an average difference of 4.45×10^{-8}. This estimate includes the uncertainties associated with the simulation, the presumption that κ equals a constant, the low Reynolds number effects on the linearity of the $\beta^{-1/2}$ distribution, and our capacity to estimate the third derivative using simple finite differences. Of course, uncertainty statements constructed in this manner also depend on the y^+ range considered.

3.3.2. *Slope of the characteristic length scale distribution*

Equation (2.10) provides a fundamental statement about the nature of the dynamical self-similarity on the L_β hierarchy. As recently pointed out to the authors by S. Guntur and F. Mehdi the product of quantities in (2.11) may be expressed in the form of a

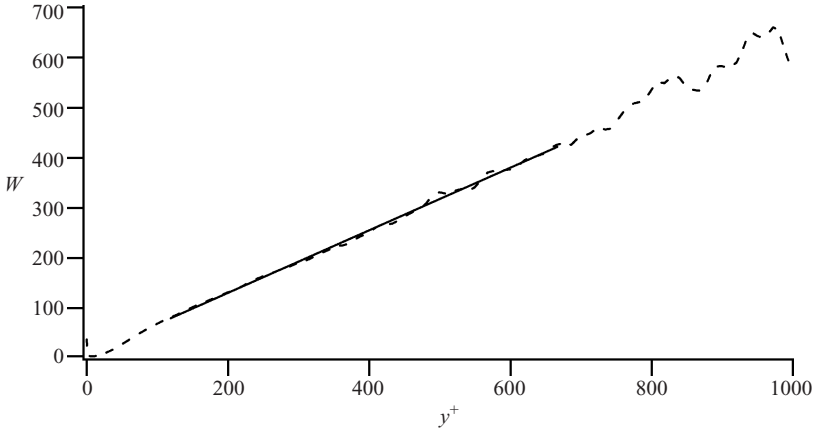

FIGURE 11. Characteristic length distribution of the L_β hierarchy in turbulent channel flow at $\delta^+ = 2003$, – – –. Linear fit ($W = 0.6247y^+ + 5.61$) of the distribution between $118 \leqslant y^+ \leqslant 667$, ——.

single derivative

$$\frac{\mathrm{d}\beta^{-1/2}}{\mathrm{d}y^+} = -\frac{1}{2}\left[\beta^{-3/2}\frac{\mathrm{d}^2T^+}{\mathrm{d}y^{+2}}\right]. \tag{3.5}$$

By virtue of (2.9) and (2.14) one finds that

$$\frac{\mathrm{d}W(y^+)}{\mathrm{d}y^+} = \frac{A}{2} = \sqrt{\kappa}. \tag{3.6}$$

Equation (3.6) conveys much about the nature of wall turbulence. For the present purposes it is perhaps most significant to note that it explicitly reveals the connection between logarithmic-like behaviour and the asymptotic linearity of the L_β width distribution, $W(y^+)$. Figure 11 re-plots the $\delta^+ = 2003$ profile of figure 5 along with a linear fit of this distribution over the range $y^+ > 2.6\sqrt{\delta^+}$, $y/\delta < \delta/3$. As can be seen, the data adhere closely, but not perfectly, to a straight line. The slope of the line is given by 0.6247 ± 0.0027, where the uncertainty is expressed as one standard deviation of the coefficient variation about its mean. This estimated slope corresponds to a prediction for the leading coefficient of $0.387 \leqslant A^2/4 \leqslant 0.394$. As with the effective derivative based estimate, this range of values is bounded by the minimum and maximum values of $(y^+\mathrm{d}U^+/\mathrm{d}y^+)^{-1}$ over the given y^+ interval. It is also worth noting that (3.6) generally constitutes a more experimentally approachable means of estimating κ than the method depicted in figure 10.

4. Discussion and conclusions

The results presented herein support the first-principles-based theory developed in Wei *et al.* (2005*a*) and Fife *et al.* (2005*a*,*b*, 2009). The existence and properties of the L_β layer hierarchy as derived from the theory are precisely demonstrated in the simulation data. Similarly, the data were shown to also strongly support the theoretically predicted features describing how and why logarithmic dependence occurs. Specifically, an explicit formula for κ was convincingly shown to hold. In its most fundamental form this equation represents the second derivative of the Reynolds stress evaluated at y_m^β on each L_β and normalized using the characteristic length on

each L_β. For the purposes of computation, other more convenient but equally valid forms (e.g. (3.6)) were employed.

The factors underlying when κ might approximate a constant are consistent with the observed robustness of logarithmic-like behaviour, as well as the long-standing difficulty of precisely determining the value of κ. The present theory makes it clear that by its very nature logarithmic dependence is approximate, and that through describing this approximate behaviour the underlying dynamical mechanisms are revealed. The constancy of κ directly measures the level of dynamical self-similarity from one L_β layer to the next. In planar channel flow, the approximate nature of κ stems from the influence of finite Reynolds number owing to the asymptotic linear behaviour of $\beta^{-1/2}$ and the likely contamination of the hierarchy from 'edge effects'. In boundary layers it results from these influences, along with the fact that unlike the $1/\delta^+$ term in (2.2) the mean advection term is not constant across the layer and develops slowly in x. The variation of this term will influence the $\beta^{-1/2}$ distribution.

A number of methods were explored relative to estimating the leading coefficient, $A^2/4$. While all of these methods are analytically equivalent, some are more amenable to computation using data. Methods stemming directly from the fundamental definition of A (defined in (2.14), (2.16) and (2.18)) were shown to exhibit considerable uncertainty. They did, however, provide evidence that A is bounded on the hierarchy and attains values close to 0.4. The effective derivative method of figure 10 produced a much less uncertain estimate, but owing to the data requirements can currently only be used in conjunction with numerical results. The length scale slope method (3.6) also exhibited low uncertainty. This computation involves a single derivative, and thus will likely prove to be more appropriate to use with experimental data. Both the effective derivative and the length scale slope method produced estimates for κ that fell between the κ bounds given by the indicator function of figure 2 over the relevant y^+ range.

A number of the implications of the present theory have been discussed in the references cited herein, and thus will not be repeated. Instead, we provide a brief set of clarifying statements.

At any given Reynolds number, logarithmic-like behaviour, if it exists, occurs owing to an approximate dynamical self-similarity on an interior domain. The existence of approximate self-similarity under such conditions has long been observed (e.g. Barenblatt 1996).

The use of the test function T^β reveals that the layer hierarchy is composed of an array of force balance breaking and exchange layers of increasing scale. In all likelihood, this property is a statistical signature having association with the dynamical evolution of hairpin-like vortices and/or vortex packets known to exist (e.g. Adrian, Meinhart & Tomkins 2000; Marusic 2001; Ganapathisubramani, Longmire & Marusic 2003; Wu & Moin 2009).

Equation (2.14) reveals that κ is a measure of the similarity between the turbulent force ($\mathrm{d}T^+/\mathrm{d}y^+$) and the gradient of this force. Equation (2.18) reveals that this same similarity condition simultaneously exists between the mean vorticity gradient and its rate of change. The equivalence of the processes by which mean momentum is transported toward the wall and mean vorticity is transported away from the wall has been rigorously shown (Eyink 2008). Other analyses indicate that the connections between these two simultaneous processes are likely to be associated with the properties of the Lamb vector ($\boldsymbol{\omega} \times \boldsymbol{u}$) and its derivatives (Hamman, Klewicki & Kirby 2008).

Equation (2.13) can be found from (2.3) and its boundary conditions via a cogent set of mathematical steps. Given the indeterminacy of (2.3), this implies its closure. Broadly speaking, closure of (2.3) requires an additional equation that relates T to U. The present theory implicitly accomplishes this on the L_β hierarchy through the similarity statement (2.10). Under perfect self-similarity $A = const$, and thus from one L_β to the next,

$$A\left(-\frac{\mathrm{d}^2U^+}{\mathrm{d}y^{+2}}\right)^{3/2} = \frac{\mathrm{d}^2T^+}{\mathrm{d}y^{+2}}. \tag{4.1}$$

This expresses a *constraint* on the profiles of U and T that supplements (2.3). The condition (4.1) is not imposed, but rather emerges as an increasingly well-approximated property of the mean dynamics as $\delta^+ \to \infty$. This is made apparent by the fact that (4.1) is not hypothesized. Instead, it is derived through the process of solving for the differential transformations that render (2.5) invariant and parameter free (i.e. (2.7)) on each L_β of the hierarchy. Among other things, this same analysis also produces a first-principles-based origin for the *distance from the wall* scaling that is often assumed in wall-flow studies.

To the authors' knowledge, the present theory is unique in its first principles based approach, and in its capacity to provide an independent and explicit equation for κ. (As noted in Fife *et al.* (2005*b*), this equation has an interesting similarity to the representation of the mixing length as the ratio of derivatives as first proposed by von Kármán (1930).) As made clear by Fife *et al.* (2009), the present theory has no apparent connection to theories based upon the hypothesis of an overlap layer as first formulated by Millikan (1939) and Izakson (1937), and as pursued by numerous researchers (e.g. see Afzal 1982; Panton 2005; Buschmann & Gad-el-Hak 2007; Monkewitz, Chauhan & Nagib 2008 and the references therein).

This work was partially supported by the National Science Foundation (CBET-0555223, grant monitor, W. Schultz) and the Office of Naval Research (N00014-08-1-0836, grant monitor, R. Joslin). The authors thank Drs Hoyas and Jimenez and Drs Kawamura, Abe and Shingai for making their simulation data available on their websites. The authors also thank the referees and editor for their recommendations.

REFERENCES

Adrian, R., Meinhart, C. & Tomkins, C. 2000 Vortex organization in the outer region of the turbulent boundary layer. *J. Fluid Mech.* **422**, 1–54.

Afzal, N. 1982 Fully developed turbulent flow in a pipe: an intermediate layer. *Ing.-Arch.* **52**, 355–377.

Barenblatt, G. 1996 *Scaling, Self-Similarity and Intermediate Asymptotics.* Cambridge University Press.

Buschmann, M. & Gad-el-Hak, M. 2007 Recent developments in scaling of wall-bounded flows. *Prog. Aerosp. Sci.* **42**, 419–467.

Cantwell, B. 2002 *Introduction to Symmetry Analysis.* Cambridge University Press.

Eyink, G. 2008 Turbulent flow in pipes and channels as cross-stream "inverse cascades" of vorticity. *Phys. Fluids* **20**, 125101.

Fife, P., Klewicki, J., McMurtry, P. & Wei, T. 2005*a* Multiscaling in the presence of indeterminacy: wall-induced turbulence. *Multiscale Model. Simul.* **4**, 936–959.

Fife, P., Klewicki, J. & Wei, T. 2009 Time averaging in turbulence settings may reveal an infinite hierarchy of length scales. *J. Discrete Continuous Dyn. Syst.* **24**, 781–807.

Fife, P., Wei, T., Klewicki, J. & McMurtry, P. 2005*b* Stress gradient balance layers and scale hierarchies in wall bounded turbulent flows. *J. Fluid Mech.* **532**, 165–189.

Ganapathisubramani, B., Longmire, E. & Marusic, I. 2003 Characteristics of vortex packets in turbulent boundary layers. *J. Fluid Mech.* **478**, 35–46.

George, W. & Castillo, L. 1997 Zero-pressure gradient turbulent boundary layer. *Appl. Mech. Rev.* **50**, 689–729.

Hamman, C., Klewicki, J. & Kirby, M. 2008 On the Lamb vector divergence in Navier–Stokes flows. *J. Fluid Mech.* **610**, 261–284.

Hansen, A. 1964 *Similarity Analyses of Boundary Value Problems in Engineering*. Prentice-Hall.

Hoyas, S. & Jimenez, J. 2006 Scaling of the velocity fluctuations in turbulent channels upto $Re_\tau = 2003$. *Phys. Fluids* **18**, 011702.

Izakson, A. 1937 On the formula for the velocity distribution near walls. *Tech. Phys. USSR* IV, **2**, 155–162.

von Kármán, T. 1930 Mechanische ahnlichkeit und turbulenz. *Nachr. Ges. Wiss. Gottingen, Math.-Phys. Klasse*. 58–76.

Kawamura, H., Abe, H. & Shingai, K. 2000 DNS of turbulence and heat transport in a channel flow with different Reynolds and Prandtl numbers and boundary conditions. In *Turbulence Heat and Mass Transfer 3 (Proceedings of the Third Intl Symp. on Turbulence Heat and Mass Transfer),* pp. 15–32. Aichi Shuppan.

Klewicki, J., Fife, P., Wei, T. & McMurtry, P. 2006 Overview of a methodology for scaling the indeterminate equations of wall-turbulence. *AIAA J.* **44**, 2475–2484.

Klewicki, J., Fife, P., Wei, T. & McMurtry, P. 2007 A physical model of the turbulent boundary layer consonant with mean momentum balance structure. *Phil. Trans. R. Soc.* A **365**, 823–839.

Marusic, I. 2001 On the role of large-scale structures in wall turbulence. *Phys. Fluids* **13**, 735–743.

Metzger, M., Adams, P. & Fife, P. 2008 Mean momentum balance in moderately favourable pressure gradient turbulent boundary layers. *J. Fluid Mech.* **617**, 107–140.

Millikan, C. B. 1939 A critical discussion of turbulent flows in channels and circular tubes. In *Proceedings of Fifth International Congress of Applied Mechanics*, pp. 386–392. Wiley.

Monkewitz, P., Chauhan, K. & Nagib, H. 2008 Comparison of mean flow similarity laws in zero pressure gradient turbulent boundary layers. *Phys. Fluids* **20**, 105102.

Moser, R., Kim, J. & Mansour, N. 1999 Direct numerical simulation of turbulent channel flow up to $Re_\tau = 590$. *Phys. Fluids* **11**, 943–945.

Nagib, H. & Chauhan, K. 2008 Variation of von Karman coefficient in cannonical flows. *Phys. Fluids* **20**, 101518.

Oberlack, M. 2001 A unified approach for symmetries in plane parallel turbulent shear flows. *J. Fluid Mech.* **427**, 299–328.

Osterlund, J., Johansson, A., Nagib, H. & Hites, M. 2000 A note on the overlap region in turbulent boundary layers. *Phys. Fluids* **12**, 1–4.

Panton, R. 2005 Review of wall turbulence as described by composite expansions. *Appl. Mech. Rev.* **58**, 1–36.

Perry, A. & Chong, M. 1982 On the mechanism of wall turbulence. *J. Fluid Mech.* **119**, 173–217.

Perry, A. & Marusic, I. 1995 A wall-wake model for the turbulence structure of boundary layers. Part 1. Extension of the attached eddy hypothesis. *J. Fluid Mech.* **298**, 361–388.

Pope, S. 2000 *Turbulent Flows*. Cambridge University Press.

Schlichting, H. & Gersten, K. 2000 *Boundary Layer Theory*. Springer.

Spalart, P., Coleman, G. & Johnstone, R. 2008 Direct numerical simulation of the Eckman layer: a step in Reynolds number, and cautious support for a log law with shifted origin. *Phys. Fluids* **20**, 101507.

Tennekes, H. & Lumley, J. 1972 A *First Course in Turbulence*. MIT Press.

Townsend, A. 1976 *The Structure of Turbulent Shear Flow,* 2nd edn. Cambridge University Press.

Wei, T., Fife, P., & Klewicki, J. 2007 On scaling the mean momentum balance and its solutions in turbulent Couette–Poiseuille flow. *J. Fluid Mech.* **573**, 371–398.

Wei, T., Fife, P., Klewicki, J. & McMurtry, P. 2005 Properties of the mean momentum balance in turbulent boundary layer, pipe and channel flows. *J. Fluid Mech.* **522**, 303–327.

Wei, T., Fife, P., Klewicki, J. & McMurtry, P. 2005 Scaling heat transfer in fully developed turbulent channel flow. *Intl J. Heat Mass Transfer* **48**, 5284–5296.

Wei, T., McMurtry, P., Klewicki, J. & Fife, P. 2005 Meso scaling of the Reynolds shear stress in turbulent channel and pipe flows. *AIAA J.* **43**, 2350–2353.

Wu, X. & Moin, P. 2009 Direct numerical simulation of turbulence in a nominally-zero-pressure gradient flat-plate boundary layer. *J. Fluid Mech.* **660**, 5–41.

Zagarola, M. & Smits, A. 1998 Mean-flow scaling of turbulent pipe flow. *J. Fluid Mech.* **373**, 33–79.